Journal of Molecular Liquids 347 (2022) 118321

Contents lists available at ScienceDirect

Journal of Molecular Liquids

journal homepage: www.elsevier.com/locate/molliq

Density functional theory and molecular dynamics simulation studies of bio-based fatty hydrazide-corrosion inhibitors on Fe (1 1 0) in acidic media

Najihah Mazlan [a], Khairulazhar Jumbri [a,b,*], Mohd Azlan Kassim [c], Roswanira Abdul Wahab [d], Mohd Basyaruddin Abdul Rahman [e]

[a] Department of Fundamental and Applied Sciences, Universiti Teknologi PETRONAS, 32610 Seri Iskandar, Perak, Malaysia
[b] Centre of Research in Ionic Liquids (CORIL), Institute of Contaminant Management (ICM), Universiti Teknologi PETRONAS, 32610 Seri Iskandar, Perak, Malaysia
[c] Research Centre for Carbon Dioxide Capture and Utilisation (CCDCU), School of Engineering and Technology, Sunway University, Bandar Sunway, 47500 Petaling Jaya, Malaysia
[d] Department of Chemistry, Faculty of Science, Universiti Teknologi Malaysia, UTM, Johor 81310, Malaysia
[e] Department of Chemistry, Faculty of Science, Universiti Putra Malaysia, 43400 UPM Serdang, Selangor, Malaysia

ARTICLE INFO

Article history:
Received 22 October 2021
Revised 7 December 2021
Accepted 10 December 2021
Available online 20 December 2021

Keywords:
Corrosion inhibitor
Molecular dynamics
Adsorption
Inhibition efficiency
Fatty hydrazide

ABSTRACT

Corrosion of metal pipelines is a huge industrial concern, with potential environmental pollution and economic loss. The implementation of a cost-effective technology in using waste palm oil as biobased corrosion inhibitors (CIs) has risen. However, the inhibition mechanism of CIs remains unclear due to the lack of comprehensive review and a small number of existing experimental data. Density functional theory (DFT) and molecular dynamics (MD) simulation provided significant insights into the adsorption mechanism. The influence of fatty hydrazide derivatives as effective CIs on ferrous (1 1 0) metal surface in 1.0 M HCl medium at a temperature ranging from 298 to 383 K was studied. DFT predicted inhibition efficacies of these CIs based on electronic/molecular properties and reactivity induced through the band gap energy between the HOMO and LUMO in the range of 7.290 to 7.480 eV. Results from MD simulation showed that the inhibition efficiency increased at low concentration of CIs (0.04 M) and increasing temperature, which was suggestive of chemical adsorption mechanism with the adsorption energy from −200 to −400 kJ/mol. . The result further suggested that thermal stability of CIs at high temperature increased due to adsorption energy of CI-metal interaction from heat supplied. All the findings were consistent with the experimental data reported earlier. Understanding the adsorption mechanism of fatty hydrazide derivatives on the metal surface could be used as a basis for future development of specific bio-based CIs for cost-effective corrosion control technology.

1. Introduction

Corrosion of steel pipeline systems caused by carbon dioxide (CO_2) and hydrogen sulfide (H_2S), microbiological activity, flow velocity, water chemistry, and oil/water composition is a major concern of the oil and gas (O & G) industry. This is because corrosion problems contribute to a substantial portion of the annual total costs for O & G companies worldwide [1]. Nonetheless, the system's damage is predominantly due to CO_2 in natural gas containing a high concentration of chloride, which creates a commonplace corrosive medium known as sweet corrosion. The reaction of metals with acidic media further degrades the strength and ductility of the pipelines. However, the present-day chemical cleaning and acid pickling of corroded mild steel pipelines in highly concentrated acid to remove scale or rust bring other operational concerns [2]. The process can be costly and environmentally dangerous if it is not well controlled.

Therefore, corrosion control is essential in combating this issue by implementing new advanced technology using green corrosion inhibitors (CIs). These cheap, biodegradable, and eco-friendly CIs can be produced from natural sources such as palm oil plants. Existing effective CIs are constructed from heterocyclic compounds containing heteroatoms of fatty hydrazide derivatives. Hydrazide derivatives are excellent CIs because of their capability to identify functional groups for adsorption on metallic surfaces. They include π-electrons, electron-donating groups, and planar structures [2]. Structural modifications of hydrazides can produce heterocyclic derivatives with active centers that facilitate adsorption onto

* Corresponding author.
E-mail address: khairulazhar.jumbri@utp.edu.my (K. Jumbri).

https://doi.org/10.1016/j.molliq.2021.118321
0167-7322/

metal surfaces. Although the less toxic and more cost-effective fatty hydrazide derivatives are highly studied CIs of O & G steel samples, their mechanism of inhibition remains unclear. There is a general lack of a comprehensive review of experimental reports in the literature. This deficiency can be addressed through computational modeling simulation to explicitly describe the adsorption mechanism of corrosion inhibition by fatty hydrazide derivatives. Such information could aid future researchers in designing effective and better heterocyclic derivatives as CIs. In fact, the future of O & G should focus on developing greener and eco-friendlier CIs.

According to the literature, Mohd *et al.* [3] reported that fatty acid hydrazides, namely, palmitate hydrazide (HD44), N-ethylidene palmitate hydrazide (HD45), and N-phenyl methylidene palmitate hydrazide (HD46) in 1.0 M HCl showed mixed inhibitor behavior towards mild steel corrosion that followed Langmuir isotherm model. The better performance of the 200 mg L^{-1} of HD46 (85%) at 308 K was ascribed to phenyl groups that delocalized *p*-electrons with empty *d*-orbital of Fe atoms. The above-said CIs reduced the corrosion rate up to 94% at minimum concentration. Abdallah *et al.* [4] synthesized a new hydrazide derivative, 2-(2-hydrazinyl-1,6-dihydro-6-oxopyrimidin-4-yl) aceto hydrazide (HD42) in 1.0 M HCl and 0.5 M H_2SO_4, which inhibited mild steel corrosion through physisorption. The CI showed a better performance of 90% at 0.05 M in HCl solution than in the H_2SO_4 medium, lowering corrosion rate up to 92% at minimum concentration.

Quraishi *et al.* [5] explored 11, 12, and 18 carbon atoms fatty hydrazides derivatives as CIs on mild steel in boiling 15% HCl acid solution using room temperature weight-loss method and potentiodynamic polarization studies found the CIs revealed a mixed type of behavior. The substances followed Temkin's adsorption isotherm with a higher inhibition efficiency in the range from 85% up to 96% at minimum concentration, 500 ppm of inhibitors. They also assessed corrosion inhibition actions of lauric hydrazide with various acids (cinnamic acid, succinic acid, nitrobenzoic acid, phthalic acid, and maleic acid) on mild steel, copper, brass, zinc, and aluminum in SO_2 and chloride atmospheres, by the same methods. They found that the 100 ppm of lauric hydrazide cinnamate displayed up to 98.7% inhibition efficiency, which followed the Temkin adsorption isotherm [6]. Toliwal and Jadav [7] also reported that fatty acids of 5-alkyl-4-phenyl-4H-[1,2,4]triazole-3-thiol phenyl hydrazides were good CIs on mild steel in 1.0 M HCl acid solution at all concentrations (100–500 ppm). This CI obeyed the Langmuir's adsorption isotherm.

Herein, this study aimed to understand further the adsorption mechanisms of C_{10}, C_{12}, C_{14}, C_{16}, and C_{18} atoms fatty hydrazide derivatives as CIs on ferrous metal surface in 1.0 M HCl. Moreover, information on the adsorption mechanisms of these CIs on a ferrous surface has yet to be reported. In this study, the calculations to comprehend the adsorption phenomena and the accompanying electronics effects were done using the density functional theory (DFT) method. The geometry optimization and subsequent electronic structure calculations were used and performed by the TmoleX program.

2. Methods

2.1. Quantum chemical calculations

The molecular mechanism of corrosion inhibition can be well explained by quantum chemical calculation. It is a valuable tool for gaining deeper insight into the adsorption phenomena and the accompanying electronics effects. The density functional theory (DFT) method calculations were employed to estimate these aspects in this study. Avogadro program was used to prepare all the studied molecules, and the TmoleX program performed geometry optimization and subsequent electronic structure calculations of the fatty hydrazide derivatives in a non-aqueous (vacuo) environment with def-SV(P).h basis set [8,9]. The functional B3LYP [10,11] and ground-state calculation were inserted under DFT setting to generate the input file. The TmoleX program visualized and calculated the molecular electronic structures. For validation of the experimental observations, the highest occupied molecular orbital energy (HOMO), lowest unoccupied molecular orbital energy (LUMO), energy gap (ΔE) were identified to calculate the different global reactivity parameters such as electron affinity (A), ionization potential (I), electronegativity (χ), chemical potential (π), global hardness (η), global softness (σ), global electrophilicity (ω) and the fraction of electrons transferred (ΔN) [12,13].

Koopman's theorem explained the calculations from the ionization energy (I) and electron affinity (A) of the assigned highest occupied molecular orbital energy (HOMO) and the lowest unoccupied molecular orbital energy (LUMO), as in Eq. (1) and Eq. (2).

$$I = -E_{HOMO} \tag{1}$$

$$A = -E_{LUMO} \tag{2}$$

HOMO implies the ability to donate electrons, known as electrophilic attack, whereas LUMO indicates its nucleophilic attack through the electron-accepting ability of a molecule. The small energy gap energy difference between LUMO and HOMO (Eq. (3)) depicts high chemical reactivity.

$$\Delta E_{GAP} = E_{LUMO} - E_{HOMO} \tag{3}$$

The study also measured several global reactivity parameters and compared them to the above-said experimental observations (χ, η, σ, π, ΔN, ω, back-donation energy and molecule–metal interaction energy). The calculation of first and second partial derivatives of energy (E) with respect to the external potential $v(r)$ and the number of electrons (N) yields the electronegativity (χ) and global hardness (η) of molecules as in Eq. (4) and Eq. (5).

$$\chi = -\pi = -\frac{\partial E}{\partial N} v(r) \tag{4}$$

$$\eta = -(\frac{\partial E}{\partial N}) 2 v(r) \tag{5}$$

where the chemical potential (π) corresponds to the first equality in Eq. (3), describing as the negative of electronegativity. The method of finite difference characterizes the calculation of μ, η, and π as follows:

$$\chi = -\frac{1}{2}(E_{HOMO} + E_{LUMO}) = \frac{1+A}{2} \tag{6}$$

$$\eta = -\frac{1}{2}(E_{HOMO} - E_{LUMO}) \text{or} = -\frac{1}{2}(E_{LUMO} + E_{HOMO}) = -\frac{1-A}{2} \tag{7}$$

$$\pi = -\frac{1}{2}(E_{HOMO} + E_{LUMO}) = -\frac{1+A}{2} \tag{8}$$

The inverse of the global hardness defines the global softness (σ) as in Eq. (9).

$$\sigma = \frac{1}{\eta} = -\frac{2}{E_{HOMO} - E_{LUMO}} \text{or} = \frac{2}{E_{HOMO} - E_{LUMO}} = \frac{2}{1-A} \tag{9}$$

Pertinently, the electronegativity and global chemical hardness determine the global electrophilicity index (ω) as follow:

$$\omega = \frac{\chi 2}{2\eta} = -\frac{\pi 2}{2\eta} \tag{10}$$

The fraction of transferred electrons (ΔN) and its associated energy (ΔE) from the corrosion inhibitor molecule (mol) to a metal surface (M) is well explained as follow:

$$\Delta N = \frac{\chi M - \chi mol}{2(\eta M + \eta mol)} = \frac{\pi mol - \pi M}{2(\eta M + \eta mol)} \quad (11)$$

$$\Delta E = \frac{(\chi M - \chi mol)2}{4(\eta M + \eta mol)} = \frac{(\pi mol - \pi M)2}{4(\eta M + \eta mol)} \quad (12)$$

The electron affinity, A is defined from the enthalpy of the reaction that is good for protonation in an acidic medium. High electron affinity leads to highly specific binding between inhibitors and metal surfaces. Ionization energy,I indicates the chemical reactivity of molecules in which small I are preferable following the high reactivity of the inhibition molecules. The global hardness, η, portrays the resistance towards the deformation of the electron cloud around the molecules. Inhibitors with lower values of η are better corrosion inhibitors due to their efficiency in electron donation to the metal. For electrophilicity index, ω measures the tendency of chemical species to gain electrons; hence low ω is superior in portraying the stability of molecules. In the case of electronegativity, χ, it predicts the inhibitive performance of molecules by attracting electrons. The electron transfer flows from the molecule at low to high electronegativity until they achieve a similar chemical potential for higher inhibition efficiency in the corrosion system.

2.2. Molecular dynamics (MD) simulations

The corrosion system composed of mild steel metal and corrosion inhibitors structure of fatty hydrazide derivatives with C_{10}, C_{12}, C_{14}, C_{16}, and C_{18} carbon atoms were constructed by the Avogadro software. The Fe (1 1 0) metal structure was chosen according to the recent experimental evidence on the effectiveness and high inhibition efficiency of the CIs [14]. Fe (1 1 0) is the most stable due to its lowest surface energy of Fe and in the order of Fe (1 1 0) < Fe (1 0 0) < Fe (1 1 1) facets [15]. The Fe (1 1 0) surface is preferable following its highest stable facet, thermodynamically, with the largest area of the Fe crystal. Besides, pure iron atoms are usually used instead of a mixture of iron with alloying elements in theoretical studies [15–18].

The activity of CIs plays a crucial role in corrosion inhibition of metals was studied through the adsorption energy and aggregation of the CIs. Four layers of Fe (1 1 0) metal were placed at the bottom of a 5.1 × 5.1 × 7.1 nm simulation box with the CI placed at the center of the box, surrounded by SPC water molecules. To mimic the actual scenario in the pipeline, the box was filled with the requisite number of water molecules and HCl ions to reach the desired 1.0 M of the acidic medium. Meanwhile, different simulation systems were constructed by varying the number of CIs molecules added to represent various concentrations ranging from 0.04 to 0.20 M at fixed 1.0 M HCl to study the aggregation of the CIs. Details of the number of molecules for different inhibitor concentrations' for different inhibitor concentrations are listed in Table A1 (Supporting Information). The GROMOS molecular force fields were adopted to represent the interaction potentials of CIs and metal, respectively [14]. Throughout the simulation, the integration step of 1.0 fs was used. The non-bonded interactions were calculated up to 1.2 nm, and Particle Mesh Ewald (PME) was applied to treat the long-range electrostatic interactions with a grid spacing of 1.2 nm and fourth-order interpolation [19]. Neighbor searching was done up to 1.2 nm and updated every five steps. The bond lengths were constrained using LINCS at fourth order [20], while the system's thermodynamic control used the V-rescale temperature and Parrinello-Rahman pressure control. The temperature coupling constant of 0.1 ps was used, and isothermal compressibility for pressure control was set to 4.5×10^{-5}. The reference pressure of 1.013 atm and a relaxation time of 2.0 ps were applied in the corrosion system.

Energy minimization was executed by performing each system with 10,000 steps of the steepest descent followed by 10,000 steps of conjugate gradients. The Fe metal layers were position restrained with a force constant of 10,000 kJ mol^{-1}. The canonical ensemble (NVT) was used to calculate the adsorption energy. The isobaric-isothermal (NPT) ensemble was introduced to observe the molecule aggregation between CIs on the metal surface. The simulations were performed for 10 ns at constant temperature for concentrations 0.04, 0.08, 0.12, 0.16, and 0.20 M, respectively. Equilibrium is reached once the dynamics manage to characterize the molecules' aggregation on the metal surface in the system and calculate their trajectories. The GROMACS package version 4.5 was used to perform all the MD simulations [21]. Each system's energy was calculated and substituted into Eq. (13).

$$E_{ads} = E_{total} - (E_{surface+solution} + E_{inhibitor}) \quad (13)$$

Herein, the binding energy of the inhibitor molecule is expressed as;

$$E_{binding} = -E_{interaction} \quad (14)$$

PyMOL visualized [22] and validated all the MD simulations against previous experimental findings to ensure consistency and accuracy.

3. Results and discussions

3.1. Quantum chemical calculations

The reactivity of the CI molecules on the metal surface reflects their inhibition efficiency in the corrosion system by observing the electronic distribution of CIs molecular orbital. Donating capability of molecules is associated with HOMO, whereas accepting capability is associated with LUMO. The geometry optimized fatty hydrazide derivatives molecules portray electron density over the entire molecules due to the conjugation effect (Fig. 1). All CIs donated their electrons to vacant d-orbitals of Fe (1 1 0) surface acceptor to form coordinate type bonds. Fig. 2 proves that the densities of both HOMO and LUMO are relatively uniform due to the integrated distribution of lone pairs in the heteroatoms from oxygen and nitrogen, resulting in higher HOMO density in adjacent zones. Therefore, the preferred active sites in releasing electrons are mainly located around heteroatoms of nitrogen and oxygen in the CIs structures. In addition, the alkyl chain region located near the heteroatoms led to high density in LUMO, indicating the preferred active sites for accepting electrons. However, the population of LUMO (Fig. 2) was markedly higher with increasing C-C length in the alkyl chain of the CIs structures. It is reasonable to assume that the heteroatoms segment in CIs molecules acts as the active site in donating electrons that form a coordinated bond with unoccupied d-orbitals of Fe (1 1 0) surface through chemisorption. In contrast, the C-C region near the heteroatoms became the dominant site to gain electrons from d-orbitals of the metal's surface through back-donating bond formation (*retro*-donation).

The capacity of molecule as a donor–acceptor contributor is gauged by the E_{HOMO} of donating electro to appropriate low energy acceptor molecules and empty molecular orbital. Meanwhile, E_{LUMO} describes the ability of molecules to accept the electrons in which a low value is preferable. From Table 1,E_{HOMO} of the five CIs showed insignificant value differences, portraying the reactivity and kinetic stability of the molecules towards the Fe (1 1 0) surface. The ΔE values affirmed the molecules' stability and reactivity to form coordi-

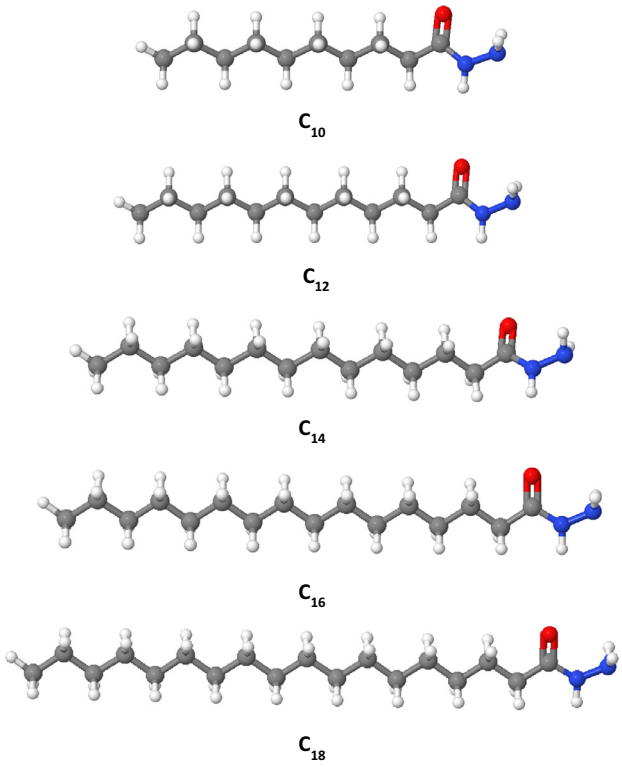

Fig. 1. Optimized structure of fatty hydrazide derivatives with different alkyl chains.

nate bonds with the d-orbitals of Fe (1 1 0) surface by donating and accepting an electron by physicochemical adsorption. The findings of this study agreed with the empirically determined potentiodynamic polarization data by Onyeachu *et al.* [23] for the adsorption of metformin drug (MET) on the C1018 steel surface in CO_2-saturated 3.5 wt% NaCl plus acetic acid. The oxidation and reduction between MET and steel surface involved the inhibitor in impeding the steel corrosion. The inhibitor competes with the hydrogen ions from acid solution for adsorption on the metal surface. In this way, the CIs block the sink and eventually consume electrons from iron oxidation through physisorption. These changes shifted the polarization corrosion potential values from −649 (without MET) to −746 mV (in 200 ppm MET). The corrosion current density reduced from 47.70 (without MET) to 4.33 μA cm^{-2} (with 200 ppm MET), confirming the MET inhibitor's inhibition efficiency as high as 86.31% by [23].

The study proved that the synthesized CIs reduced Fe (1 1 0) corrosion by existing as a protonated species in the solution. This fact corresponds with the current study in which the fatty hydrazide derivatives' alkyl chain was the protonated species in the corrosion system. The data also corroborated that the inhibitors' stable, relative inhibition efficiencies in the presence of an alkyl chain. The data proved that the corrosion inhibitions were by physisorption and chemisorption despite having heteroatoms in the structure. Therefore, lesser energy is required to remove an electron from the last occupied molecular orbital for polarization electron transport due to the CIs' structural stability.

Table 1 also shows the value of electron affinity (*A*) and ionization potential (*I*) of the inhibitors. The affinity values for all inhibitors were insignificantly different, in the range of −0.463 up to −0.300. The data indicated high electron affinity that led to the highly specific binding between inhibitors and metal surfaces. In this context, the results were in line with electrochemical impedance spectroscopy (EIS) reported by Khowdiary *et al.* [24]. EIS profile of disposed of polyethylene terephthalate (PET), namely W-PET-1,W-PET-2, and W-PET-3 compounds in 0.5 M H_2SO_4, recognized by the surface in-homogeneities and roughness of carbon steel was due to the inhibitors' protective layer on the carbon steel surface. The synthesized inhibitors enhanced the transfer resistance in the acidic solution without modifying the dissolution progress. The behavior seen here can be accredited to the adsorption of inhibitors on the carbon steel surface through the high affinity of strong electron charge transfer between CIs and metal surfaces. The interaction increases the CIs efficiency in the acidic solution.

Therefore, the good correlation with the previous experimental studies from Khowdiary *et al.,* [24] proves that the adsorption of inhibitors on metal surface coinciding between alkyl chain and electron donors on heteroatoms were allotted to electrochemical responses in the corrosion system through mixed-type behavior. In addition, the values of *I* showed a slight difference in which the values were small enough, between 6.998 up to 7.023, to increase the chemical reactivity of the CIs that eventually raised the inhibition efficiency. Vosta *et al.,* [25] described that corrosion inhibition efficiency increases with reducing ionization potential. Inhibitors with the highest energy have the least firmly bonded electrons in the HOMO orbital. In this context, corrosion reaction can be blocked from HCl acid medium when the inhibitors molecules act as an electron donor to the metal surface, forming a surface layer to block the corrosion.

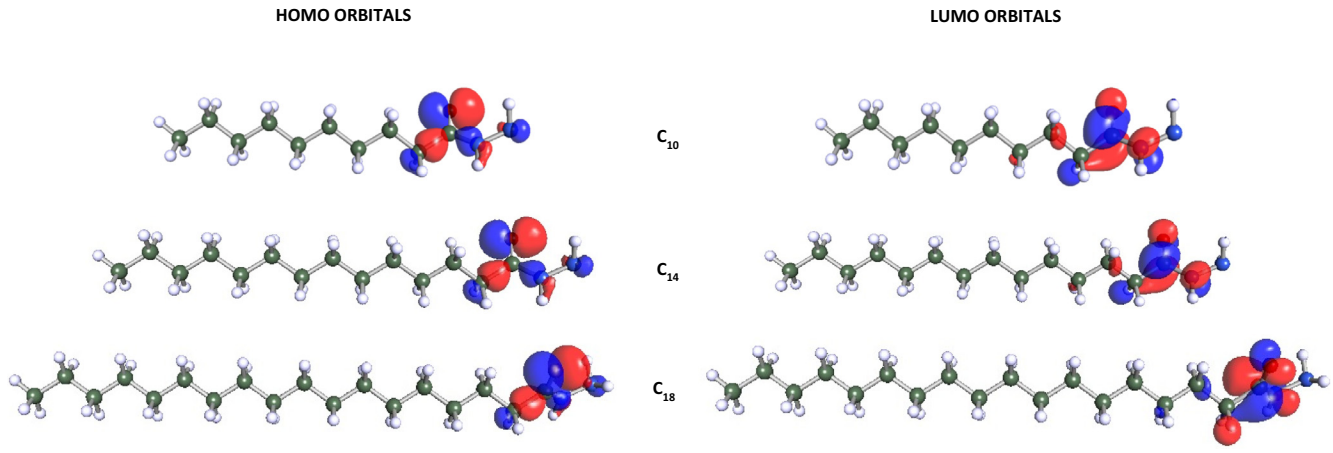

Fig. 2. HOMOs and LUMOs of non-protonated inhibitor molecules using DFT/B3LYP.

Table 1
Selected quantum chemical parameters for the studied fatty hydrazide derivatives.

CIs	E_{HOMO} (eV)	E_{LUMO}(eV)	ΔE(eV)	I	A	η	χ	ΔN
C_{10}	− 7.021	0.460	7.480	7.021	− 0.460	3.280	3.740	−0.497
C_{12}	− 6.998	0.300	7.290	6.998	− 0.300	3.351	3.647	−0.500
C_{14}	− 7.018	0.463	7.480	7.018	− 0.463	3.278	3.740	−0.497
C_{16}	− 7.015	0.463	7.480	7.015	− 0.463	3.276	3.739	−0.497
C_{18}	− 7.023	0.449	7.470	7.023	− 0.449	3.287	3.736	−0.496

Likewise, the χ of the hydrazide CIs exhibited a good correlation with the electron transfer, indicating that electron transfer started from low to high electronegativity until a similar chemical potential was achieved. From there, the fraction of electron transferred (ΔN) from the CIs molecules to the metal surface can be calculated. Lukovits *et al.,* [26] reported that ΔN can be referred to as 'electron-donating ability", representing the number of electrons that will be donated and accepted between the CIs and metal surface. In this study, the theoretical values used for χ_{Fe} (7.0 eV) and η_{Fe} (0.0 eV) were adopted from literatures [27–30]. The ΔN data in Table 1 shows there is only a slight difference for all the CIs, −0.500 up to −0.496. These negative values are $\Delta N < 3.6$, indicating that electron-donation occurred from the metal surface to the optimized structure in the corrosion system. Rani *et al.* [31] stated that excellent corrosion inhibitors also involved *retro*-donation despite donating electrons to the unoccupied orbital of the metal. Previous studies reported that ΔN values could result either from electron donation of heteroatoms to the metal. This behavior proves that chemisorption occurred by forming a coordinate bond, or metal to the molecules, portraying *retro*-donation [32,33].

Zhang *et al.* [34] also mentioned improvement in inhibition efficiencies, mainly from the electron-donating ability to the metal surface. Hence, the ability of fatty hydrazide derivatives to donate electrons to the metal surface supported the findings by Zhang *et al.* [34] in yielding a good inhibitory effect for corrosion system by electron donation of heteroatoms to the unoccupied d-orbital of iron and vice versa. The electrochemical tests also showed that the nitrogen atoms in imidazole and pyridine rings of 2-(4-pyridyl)-benzimidazole (PBI) in 1.0 M HCl on the metal steel favored the formation of a Fe(II)-PBI complex. This modification of the dissolution mechanism of iron through chemisorption was due to an electron donation from lone pair of electrons in the nitrogen atom, elevating the corrosion system's inhibition efficiency. Notably, the experimental report indicated a good correlation with this study of fatty hydrazide derivatives being good corrosion inhibitors. Hence, the obtained ΔN values were valid to support chemisorption as the vital process during corrosion inhibition.

Global hardness (η) has also been used as a molecular descriptor of selectivity and reactivity based on the Lewis theory of acid and bases. The η values for all CIs exhibited slight differences, with values between 3.276 up to 3.287, signifying their similar hardness and high inhibition efficiency. This was due to the CIs' high proficiency in donating an electron to the metal surface, preventing the resistance towards the electron cloud deformation. The frontier molecular orbitals and orbital energies data collectively proved that the inhibition efficiency correlated well with the CIs' ability to accept electrons from the Fe (1 1 0) surface and vice versa. The values thereby demonstrated the mixed-type inhibitors in this study. Boughoues *et al.,* [35] reported that nitrogen atom in amine derivatives inhibitors on Fe (1 1 0) in 1.0 M HCl enhances the corrosion inhibition performance by facilitating the electrons transfer to the vacant Fe-orbital by obeying the Langmuir isotherm. In another work by Kumari *et al.* [2] on polarization also revealed a mixed-type 2-[(2-methylquinolin-8-yl)oxy] acetohydrazide (HD47) inhibitors in HCl (0.5 and 1.0 M) media towards mild steel. The findings followed the Langmuir adsorption isotherm model that reduces the corrosion rate by 76%. Polarization studies and weight loss method from Quraishi *et al.,* [5] on fatty thiosemicarbazide derivatives on Fe (1 1 0) in 1.0 M HCl also proved the compounds' mixed behavior was mainly due to the presence of heteroatoms in the moieties of CI molecules contributed that contributed electrons to the metal surface, raising inhibition efficiency 17.1% to 97.4%.

3.2. Molecular dynamic (MD) simulation

3.2.1. Adsorption energy

The interaction between the active sites of CI-based fatty hydrazides and Fe (1 1 0) surface was explained using MD simulation. A deeper understanding of the interaction between each inhibitor and metal surface was gained through visual simulation of the corresponding adsorption mechanism of the CIs. Their different adsorption energies with different alkyl chains and metal surfaces, Fe (1 1 0), are illustrated in Fig. 3. The results supported a chemisorption process since the adsorption energies (E_{ads}) were between −200 to −400 kJ/mol [36]. As predicted, the adsorption energy increases when the length of the alkyl chain increases. The increase in chain length increases the tendency of the hydrophobic tail to displace surface water molecules and improves attraction towards the metal atom. Furthermore, the adsorption energy became increasingly negative with increasing temperature (Fig. 3), reflecting the exothermic nature of the chemisorption process. Hence, higher performance of the fatty hydrazide CIs were expected at high temperatures. Such behavior can be interpreted on the basis that desorption of adsorbed inhibitor molecules from the Fe (1 1 0) surface would not happen with the temperature rise.

The simulation result was in good agreement with a previous report by Bouassiriaa *et al.* [36] for corrosion inhibitors 5-(4-methylpiperazinyl)-methylquinolin-8-ol (MPMQ). The CI showed a ∼ 95% inhibition performance on carbon steel in 1.0 M HCl

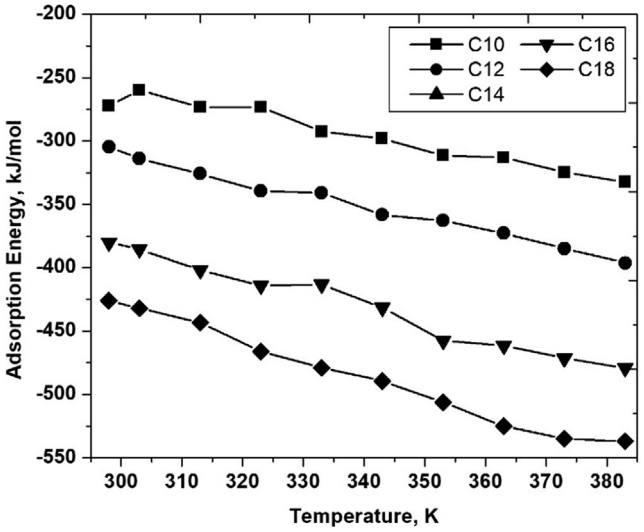

Fig. 3. The adsorption energy of corrosion inhibitors at different alkyl chains with temperatures between 298 and 383 K.

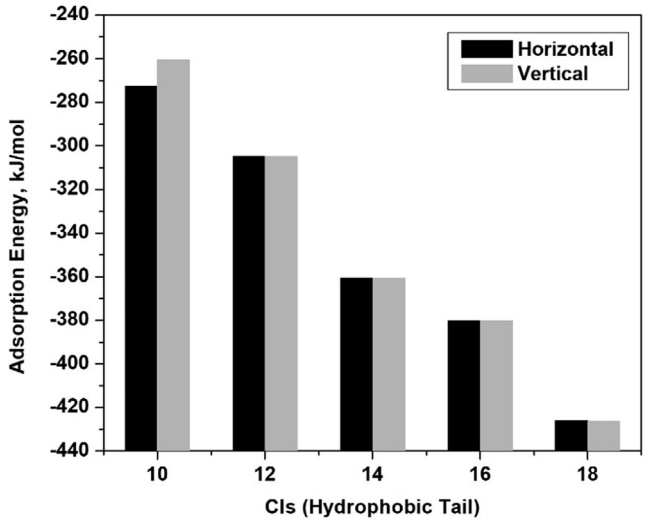

Fig. 4. The adsorption energies of CIs at different alkyl chains and orientations.

because of the heteroatoms' electron-donating groups that increased the electron density around the CI adsorption sites. The heteroatoms provided additional anchoring sites for CI-metallic adsorption with increasing temperatures from 298 to 328 K. They also mentioned that the chemisorption process in their study was well-explained and proven through XPS analysis. The diffractogram revealed chemical interaction between inhibitors on the exposed area of mild steel due to heteroatoms such as C = O and C-O-H groups.

Furthermore, inhibition efficiency of CIs reported by Gomma *et al.* [37] improved with increasing temperature, which delayed the corrosion rate. This finding is associated with the diffusion process in which the number of CIs reaching the metallic surface is greater at a higher temperature than at lower temperature conditions. This indicates that higher activation energy is available for adsorption processes with a risinh electron density in the vicinity of the adsorption centers. These changes favor the higher diffusion rates of CIs, leading to high inhibition efficiency. Therefore, our findings suggest that the number of adsorption sites, mode of interaction between CI-metal surface, the charge density of alkyl chain, and the lone pair of heteroatoms were the factors influencing adsorption efficiency of CIs, hence agreeing with findings by Bouassiriaa *et al.* [36].

The adsorption abilities of CIs on Fe (1 1 0) surface can be translated to binding energy that can indicate the performance of studied inhibitors against metal corrosion. The binding energy values were positive, indicating easy adsorption on the metal surface, with the CIs' inhibition efficiency affected by the length of the alkyl chain. In this study, the CIs performance was observed in the following order: $C_{10} < C_{12} < C_{14} < C_{16} < C_{18}$. It was shown that the inhibition efficiency inhibited a higher negative value of adsorption energy ranging from −72.306 to −426.003 kJ/mol. These values were consistent with the DFT calculation as discussed previously, suggesting a chemical adsorption mechanism. The order was compatible with inductive effects of the heteroatom moieties (N and O) of the CIs adsorbed on the metal surface in a near-horizontal orientation, portraying their optimum interactions with the Fe (1 1 0) surface. In addition, the presence of lone pair on the nitrogen atom causes the CI molecule to be more polarizable for an easy donation of electrons to the metal surface. The inductive effect of the heteroatoms also influenced the calculated binding energies. This proved that the adsorption energy was comparable to potentiodynamic polarization, where the value of corrosion energy affects the inhibition efficiency. The negative value seen here proved that the CIs hindered the transfer of H^+ ions from HCl towards metal, facilitated by the presence of the protective film on the metal surface. The protective film formation enhanced the adsorption process by transferring the electrons to form a chemical bond with the metal surface [38]. As the alkyl chain increases, the higher the adsorption energy as the alkyl chain contributes to replacing water molecules, thus increasing binding ability. The highest magnitude of adsorption energy was obtained for C_{18}, proving that C_{18} has the strongest interaction with Fe (1 1 0).

The horizontal orientation of the CIs on the Fe (1 1 0) surface portrays how the CIs can minimize the contact area between corrosive elements and metal surfaces in a corrosive environment of HCl. Fig. 4. shows that horizontal orientation inhibited higher adsorption energy for C10 inhibitor and the insignificant difference with the increasing alkyl chain length in the corrosion inhibitor's

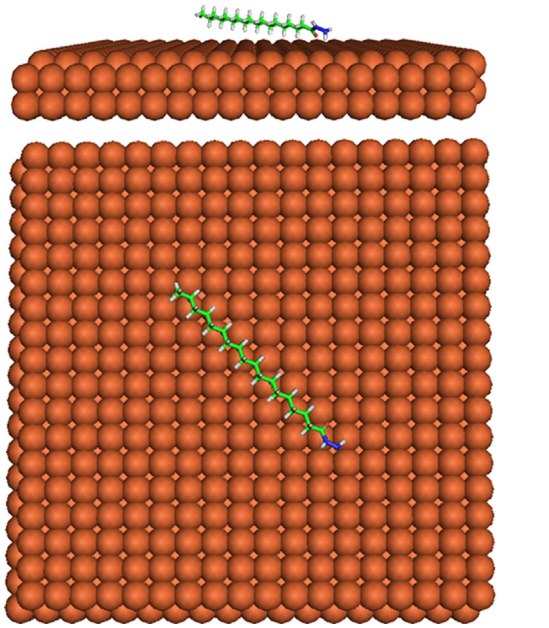

Fig. 5. Top and side view of adsorption configurations of fatty hydrazide inhibitor (C_{18}) on Fe (1 1 0) in 1.0 M HCl environment·H_2O molecules and ions were removed for clarity.

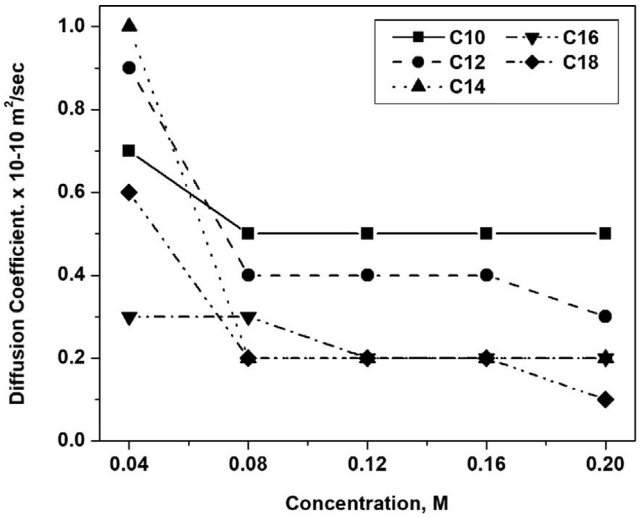

Fig. 6. Diffusion trend of corrosion inhibitors at different alkyl chains with increasing concentration ranging from 0.04 to 0.20 M.

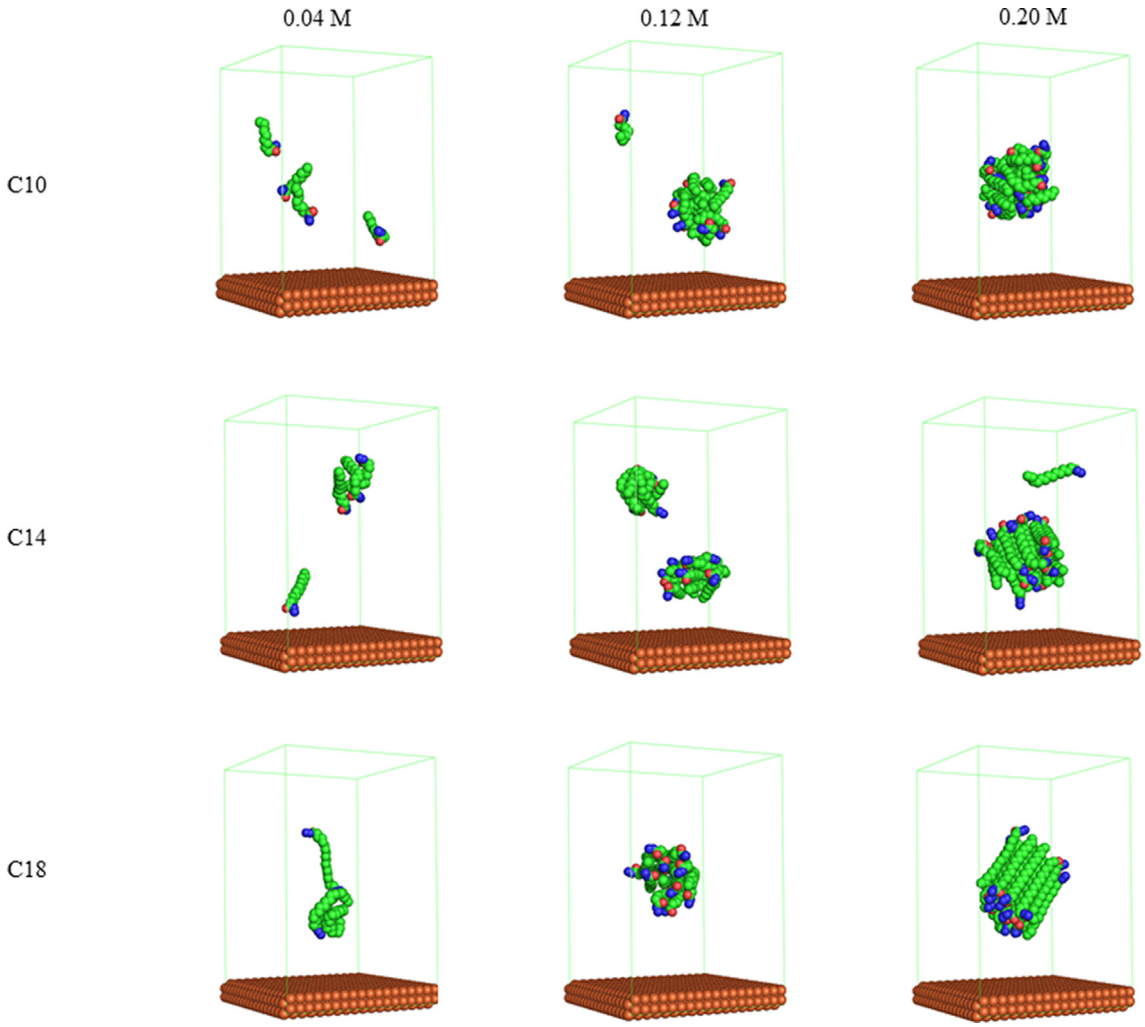

Fig. 7. Cluster size at different alkyl chains of inhibitors with different concentrations at 10 ns, H_2O molecules, and ions were removed for structures clarity in the vacuum phase.

structure. The Monte Carlo (MC) simulation study on MPMQ inhibitors by Bouassiria *et al.*, [36] showed that they adsorbed similarly on the Fe surface. The interaction led to high negative adsorption energy values of −1149 kJ/mol, indicating chemisorption process with maximal metal surface coverage by the corrosion inhibitors. In addition, Verma *et al.*, [39] reported that sodium 2-quinoxalinecarboxylate inhibitor on a Fe substrate with a planar orientation is preferred for better inhibition performance in the corrosion system because it covers a larger surface area of metal with a higher binding energy. Therefore, C_{10}-fatty hydrazide derivative in this study was in line with previous computational works in portraying high inhibition efficiency with a planar orientation as in Fig. 5.

3.2.2. Molecular aggregation

Fig. 6 shows the diffusion coefficient of CI molecules at various concentrations. The diffusion trend of inhibitors was high at a low concentration of 0.04 M. The trend seen here agreed with the experimental finding reported by Quraishi *et al.* [40], where lauric hydrazide (LH) inhibitor enhanced the inhibition efficiency (IE) as high as 87% even at a low concentration of 250 ppm of LH. This was due to an interaction of metal and inhibitor molecules that formed a physical barrier between the corrosive environment and the metal surface. It can be proven in this study where the diffusion trend of CIs decreases with increasing concentration. C_{10} molecules diffused faster than C_{12}, followed by C_{14}, $C_{16,}$ and C_{18} due to the increasing number of molecules in increasing inhibitors concentration. The diffusion trend decreased due to clusters formation of corrosion inhibitors in the system over high concentration, as the number of molecules increases. Aggregation of molecules occurs in the system due to the increasing molecule cluster size, thus reducing CIs diffusion and adsorption to the metal surface. As reported by Xia *et al.* [41], the inhibition efficiency of a CI decreases with the increasing concentration of inhibitor, as observed from gravimetric measurement and potential polarization curves.

Findings from the MD simulation also corresponded well with the DFT calculation discussed previously. In this study, all CIs exhibited decreasing diffusion trend with increasing concentration due to the formation of clusters with the increasingly hydrophobic C_{14}, $C_{16,}$ and C_{18} alkyls. These molecules rapidly aggregated compared to C_{10} and C_{12}. However, the CIs showed better inhibitory performance at 0.04 M as no cluster aggregation was observed (Fig. 7). The outcome seen here correlated linearly with previous experimental findings on electrochemical impedance data reported by Chakravarthy *et al.* [42] for nicotinamide derivatives for concentrations 200 to 500 ppm in 0.5 M HCl solution. They found that the double layer capacitance decreases, and polarization resistance (RP) increases as the concentration of the inhibitors increases from 303 to 333 K. A reduction in diffusion coefficient

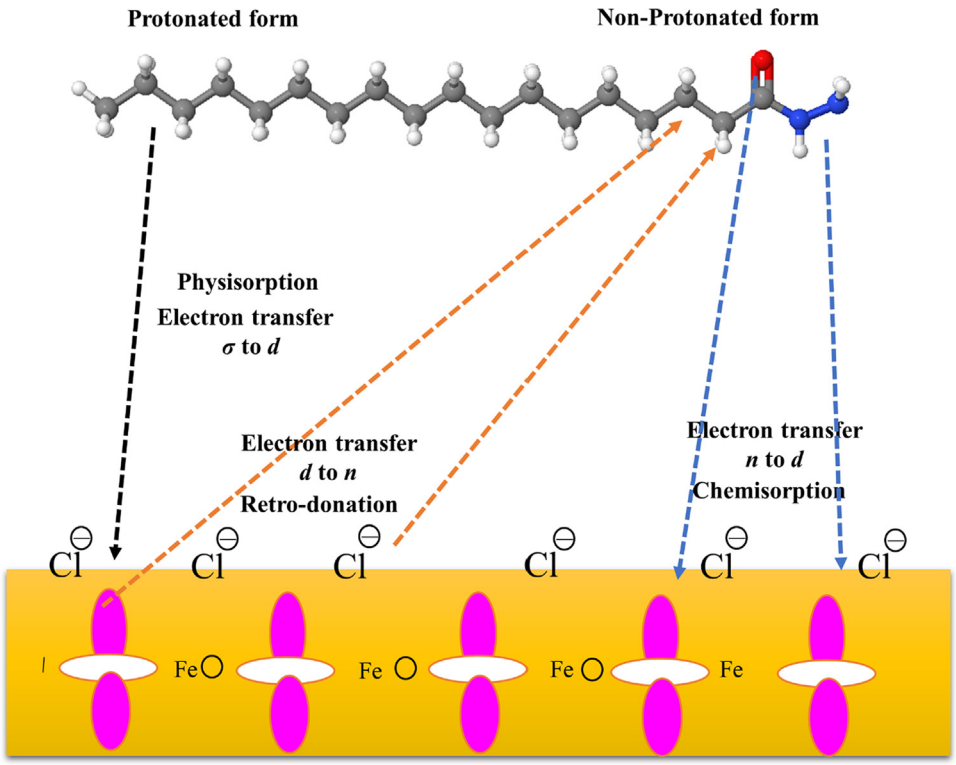

Fig. 8. Schematic illustration of the adsorption mechanism of fatty hydrazide derivatives CIs on Fe (1 1 0) surface in a 1.0 M HCl solution.

was a consequence of both the concentration and aggregation effects. It was also observed that all the CIs aggregate in clusters of diameters greater than half the box length at high concentrations, forming system-spanning micelles. Pertinently, this study's computational findings mirrored the earlier results by Zhang *et al.* [34].

3.2.3. Mechanism of adsorption and inhibition

The adsorption mechanism of the CI-metallic interaction in 1.0 M HCl is illustrated in Fig. 8. The Fe (1 1 0) surface experienced rapid oxidation in an aggressive environment and adopted a positively charged metal surface. This is in turn, caused the negatively charged counter chloride ions to form a negatively charged layer over the metallic surface by electrostatic attraction. The addition of CI into the system resulted in physisorption. The protonated inhibitor molecules bind to the negatively charged metal surface. This was followed by electrons donation by the lone pair electrons of unprotonated nitrogen and oxygen atoms in the CI to the vacant *d*-orbitals of the Fe-atom, leading to chemisorption. The accumulation of electron clouds might occur during the electron transfer, resulting in inter-electron repulsions. Subsequently, *retro*-donation of electron transfer from *d*-orbital to the unoccupied molecular orbitals of the CI must take place to reinforce the adsorption of the CI on the metal surface.

In this study, the expected adsorption, physisorption, chemisorption, and *retro*-donation processes also transpired in the adsorption mechanism of the fatty hydrazide derivatives CIs on the Fe (1 1 0) metal surface. The above outcome was due to the CIs mixed type behaviors, which concurred with the previous computational work reported by Bouassiria *et al.*, [36]. The simulated 5-(4-methylpiperazinyl)-methylquinolin-8-ol (MPMQ) also showed a mixed-type behavior in 1.0 M HCl. Protonated MPMQ molecules interacted through physisorption via adsorbed Cl^- ions after forming positive charges on the metal steel through electrostatic attractions between Cl^- ions in HCl solution. Chemisorption also occurred via Fe-unfilled orbitals by electron donated from the lone pairs in heteroatoms of MPMQ and π electrons via Fe empty orbitals.

4. Conclusion

In this study, DFT calculations showed a good correlation with experimental and molecular dynamics simulation. Molecular quantum chemical calculations revealed that the reactive sites mainly from N and O-atoms affected the inhibition efficiency of CIs on the corrosion of Fe (1 1 0). The adsorption mechanism in terms of energy, aggregation, and self-assembly of CIs on mild steel surface in bulk aqueous met the Langmuir isotherm expectation. The low and negative adsorption energies of between −200 to −400 kJ/mol at low concentration of CIs were estimated at 0.04 M, in planar orientation. The data proved the fatty hydrazide derivatives as effective biobased CIs on Fe (1 1 0). The inhibition efficiency ranking of the studied CIs in preventing iron corrosion was identified in the following order of hydrazide derivatives: C_{10}- > C_{12} > C_{14} > C_{16} > C_{18}. The C_{10} hydrazide derivative was estimated to be the most effective inhibitor against the corrosion of the Fe metal surface. MD simulations revealed that these fatty hydrazide derivatives have strong binding and interactions with Fe (1 1 0) surface. The quantum calculation and MD simulation outcomes could therefore be used a future reference in the respective field.

CRediT authorship contribution statement

Najihah Mazlan: Conceptualization, Methodology, Validation, Formal analysis, Investigation, Writing – original draft, Visualization. **Khairulazhar Jumbri:** Conceptualization, Methodology, Software, Validation, Formal analysis, Resources, Writing – review & editing, Supervision, Funding acquisition. **Mohd Azlan Kassim:** Methodology, Validation, Visualization. **Roswanira Abdul Wahab:**

Software, Validation, Writing – original draft, Writing – review & editing. **Mohd Basyaruddin Abdul Rahman:** Validation, Writing – review & editing.

Declaration of Competing Interest

The authors declare that they have no known competing financial interests or personal relationships that could have appeared to influence the work reported in this paper.

Acknowledgment

This research was funded by the PETRONAS Research Sdn Bhd and Universiti Teknologi PETRONAS (GR&T UTP) Collaboration (Grant Number 015MD0-085).

References

[1] L.T. Popoola, A.S. Grema, G.K. Latinwo, B. Gutti, A.S. Balogun, Corrosion problems during oil and gas production and its mitigation, Int. J. Ind. Chem. 4 (2013) 35.
[2] P. Kumari, P. Shetty, S.A. Rao, Corrosion inhibition effect of 4-hydroxy-n′-[(e)-(1h-indole-2-ylmethylidene)] benzohydrazide on mild steel in hydrochloric acid solution, Int. J. Corros. 2014 (2014) 1–11.
[3] N.K. Mohd, M.J. Ghazali, S.K. Yeong, N.A. Ibrahim, W.M.Z.W. Yunus, S.M.M. Nor, Z. Idris, Corrosion inhibition of mild steel in hydrochloric acid solution using fatty acid derivatives, J. Oil Palm Research 29 (2017) 97–109.
[4] Z.A. Abdallah, M.S. Mohamed Ahmed, M.M. Saleh, Organic synthesis and inhibition action of novel hydrazide derivative for mild steel corrosion in acid solutions, Mater. Chem. Phys. 174 (2016) 91–99.
[5] M.A. Quraishi, D. Jamal, M. Tariq Saeed, Fatty acid derivatives as corrosion inhibitors for mild steel and oil-well tubular steel in 15% boiling hydrochloric acid, J. Am. Oil Chem. Soc. 77 (3) (2000) 265–268.
[6] M.A. Quraishi, V. Bhardwaj, J. Rawat, Prevention of metallic corrosion by lauric hydrazide and its salts under vapor phase conditions, J. Am. Oil Chem. Soc. 79 (6) (2002) 603–609.
[7] S.D. Toliwal, K. Jadav, Fatty acid triazoles derived from Neem, Rice bran, Karanja oils as corrosion inhibitors for mild steel, Indian, J Chem. Technol. 16 (2009) 32–37.
[8] M.D. Hanwell, D.E. Curtis, D.C. Lonie, T.V.E. Zurek, G.R. Hutchison, Avogadro: An advanced semantic chemical editor, visualization, and analysis platform, J. Cheminformat. 4 (2012) 17.
[9] C. Steffen, K. Thomas, U. Huniar, A. Hellweg, O. Rubner, A. Schroer, Software news and updates TmoleX-a graphical user interface for TURBOMOLE, J. Comput. Chem. 31 (2010) 2967–2970.
[10] A.D. Becke, Density-functional thermochemistry. III. The role of exact exchange, J. Chem. Phys. 98 (7) (1993) 5648–5652.
[11] A.D. Becke, Density functional calculations of molecular bond energies, J. Chem. Phys. 84 (8) (1986) 4524–4529.
[12] A.S. Fouda, Influence of some thiophene derivatives on the corrosion of iron in nitric acid solution, Monatsh. Chem. 117 (1986) 159-165.
[13] H. Allal, Y. Belhocine, E. Zouaoui, Computational study of some thiophene derivatives as aluminium corrosion inhibitors, J. Mol. Liq. 265 (2018) 668–678.
[14] N.I.N. Haris, S. Sobri, Y.A. Yusof, N.K. Kassim, An Overview of molecular dynamics simulation for corrosion inhibition of ferrous metals, Metals 11 (2020) 46.
[15] D. Douche, H. Elmsellem, E.H. Anouar, L. Guo, B. Hafez, B. Tüzün, A.E. Louzi, K. Bougrin, K. Karrouchi, B. Himmi, Anti-corrosion performance of 8-hydroxyquinoline derivatives for mild steel in acidic medium: Gravimetric, electrochemical, DFT and molecular dynamics simulation investigations, J. Mol. Liq. 308 (2020) 113042.
[16] M.P. Asfia, M. Rezaei, G. Bahlakeh, Corrosion prevention of AISI 304 stainless steel in hydrochloric acid medium using garlic extract as a green corrosion inhibitor: electrochemical and theoretical studies, J. Mol. Liq. 315 (2020) 113679, https://doi.org/10.1016/j.molliq.2020.113679.
[17] S. Chen, B. Zhu, X. Liang, Corrosion inhibition performance of coconut leaf extract as a green corrosion inhibitor for X65 steel in hydrochloric acid solution, Int. J. Electrochem. Sci. 15 (2020) 1–15.
[18] J. Liu, Y. Zhou, C. Zhou, H. Lu, 1-phenyl-1H-tetrazole-5-thiol as corrosion inhibitor for Q235 steel in 1 M HCl medium: Combined experimental and theoretical researches, Int. J. Electrochem. Sci. 15 (2020) 2499–2510.
[19] T. Darden, D. York, L. Pedersen, Particle mesh Ewald: An N·log(N) method for Ewald sums in large systems, J. Chem. Phys. 98 (1993) 10089.
[20] B. Hess, H. Bekker, H.J.C. Berendsen, J.G.E.M. Fraaije, LINCS: a linear constraint solver for molecular simulations, J. Comp. Chem. 18 (1997) 1463–1472.
[21] S. Pronk, S. Páll, R. Schulz, P. Larsson, P. Bjelkmar, R. Apostolov, M.R. Shirts, J.C. Smith, P.M. Kasson, D.V.D. Spoel, B. Hess, E. Lindahl, GROMACS 4.5: A high-throughput and highly parallel open source molecular simulation toolkit, Bioinformatics 29 (2013) 845–854.
[22] PyMOL The PyMOL Molecular Graphics System, Version 1.2r3pre, Schrödinger, LLC.
[23] I.B. Onyeachu, S. Abdel-Azeim, D.S. Chauhan, M.A. Quraishi, Electrochemical and computational insights on the application of expired metformin drug as a novel inhibitor for the sweet corrosion of C1018 steel, ACS Omega 6 (1) (2021) 65–76.
[24] M.M. Khowdiary, A.A. El-Henawy, A.M. Shawky, N.A. Negm, Synthesis and evaluation of novel corrosion inhibitors utilized from the recycling of polyethylene terephthalate polymer: Gravimetric, electrochemical, quantum chemical modeling, and molecular docking studies, J. Mol. Liq. 320 (2020) 114504.
[25] J. Vosta, J. Eliásek, Study on corrosion inhibition from aspect of quantum chemistry, Corros. Sci. 11 (4) (1971) 223–229.
[26] I. Lukovits, E. Kalman, F. Zucchi, Corrosion inhibitors-correlation between electronic structure and efficiency, Corros. 57 (2001) 3–8.
[27] V.S. Sastri, J.R. Perumareddi, Molecular orbital theoretical studies of some organic corrosion inhibitors, Corros. 53 (8) (1997) 617–622.
[28] M.J.S. Dewar, W. Thiel, Ground states of molecules. The MNDO method. Approximations and parameters, J. Am. Chem. Soc. 99 (1977) 4899–4907.
[29] F. Shojaie, N. Mirzai-Baghini, Molecular dynamics and density functional theory study on the corrosion inhibition of austenitic stainless steel in hydrochloric acid by two pyrimidine compounds, Int. J. Ind. Chem. 6 (4) (2015) 297–310.
[30] A.Y. Musa, A.A.H. Kadhum, A.B. Mohamad, M.S. Takriff, Experimental and theoretical study on the inhibition performance of triazole compounds for mild steel corrosion, Corros. Sci. 52 (10) (2010) 3331–3340.
[31] B.E.A. Rani, B.B.J. Basu, Green inhibitors for corrosion protection of metals and alloys: An overview, Int. J. Corros. 2012 (2012) 1–15.
[32] A. Kokalj, S. Peljhan, M. Finšgar, I. Milošev, What determines the inhibition effectiveness of ATA, BTAH, and BTAOH corrosion inhibitors on copper?, J Am. Chem. Soc. 132 (2010) 16657–16668.
[33] N. Kovačević, A. Kokalj, DFT study of interaction of azoles with Cu (111) and Al (111) surfaces: Role of azole nitrogen atoms and dipole–dipole interactions, J. Phys. Chem. C 115 (2011) 24189–24197.
[34] F. Zhang, Y. Tang, Z. Cao, W. Jing, Z. Wu, Y. Chen, Performance and theoretical study on corrosion inhibition of 2-(4-pyridyl)-benzimidazole for mild steel in hydrochloric acid, Corros. Sci. 61 (2012) 1–9.
[35] Y. Boughoues, M. Benamira, L. Messaadia, N. Bouider, S. Abdelaziz, Experimental and theoretical investigations of four amine derivatives as effective corrosion inhibitors for mild steel in HCl medium, RSC Adv. 10 (40) (2020) 24145–24158.
[36] M. Bouassiria, T. Laabaissi, F. Benhiba, M. El Faydy, H. Fakhry, H. Oudda, M. Assouag, R. Touir, A. Guenbour, B. Lakhrissi, I. Warad, A. Zarrouk, Corrosion inhibition effect of 5-(4-methylpiperazine)-methylquinoline-8-ol on carbon steel in molar acid medium, Inorg. Chem. Comm. 123 (2021) 108366.
[37] G.K. Gomma, M.H. Wahdan, Schiff bases as corrosion inhibitors for aluminium in hydrochloric acid solution, Mater. Chem. Phys. 39 (1995) 209–213.
[38] M. Murmu, S.K. Sahaa, P. Bhaumickc, N.C. Murmu, H. Hirani, P. Banerjee, Corrosion inhibition property of azomethine functionalized triazole derivatives in 1 mol L^{-1} HCl medium for mild steel: Experimental and theoretical exploration, J. Mol. Liq. 313 (2020) 113508.
[39] C. Verma, H. Lgaz, D.K. Verma, E.E. Ebenso, I. Bahadur, M.A. Quraishi, Molecular dynamics and Monte Carlo simulations as powerful tools for study of interfacial adsorption behavior of corrosion inhibitors in aqueous phase, A Review, J. Mol. Liq. 260 (2018) 99–120.
[40] M.A. Quraishi, D.S. Chauhan, F.A. Ansari, Development of environmentally benign corrosion inhibitors for organic acid environments for oil-gas industry, J. Mol. Liq. 329 (2021) 115514, https://doi.org/10.1016/j.molliq.2021.115514.
[41] S. Xia, M. Qiu, L. Yu, F. Liu, H. Zhao, Molecular dynamics and density functional theory study on relationship between structure of imidazoline derivatives and inhibition performance, Corros. Sci. 50 (7) (2008) 2021–2029.
[42] M.P. Chakravarthy, K.N. Mohana, Adsorption and corrosion inhibition characteristics of some nicotinamide derivatives on mild steel in hydrochloric acid solution, Int. Sch. Research Notices 13 (2014) 687276.